Charge Transport Properties of High-Strength, High-Modulus Sulfonated Polyaniline/Poly(*p*-phenylene terephthalamide) Fibers

W.-P. Lee,[†] K. R. Brenneman,[‡] C.-H. Hsu,[||] H. Shih,[||] and A. J. Epstein*[,†,‡,§]

Department of Physics, The Ohio State University, Columbus, Ohio 43210-1106; Chemical Physics Program, The Ohio State University, Columbus, Ohio 43210-1185; Department of Chemistry, The Ohio State University, Columbus, Ohio 43210-1185; and Central Research and Development, Experimental Station, DuPont Company, Wilmington, Delaware 19880

Received August 30, 2000; Revised Manuscript Received December 21, 2000

ABSTRACT: Temperature-dependent direct current (dc) and microwave (mw) conductivity, σ_{dc} and σ_{mw}, electron paramagnetic resonance (EPR), and mechanical properties of sulfonated polyaniline/poly(*p*-phenylene terephthalamide) (SPAN/PPD-T) composite fibers are presented. Tenacity and modulus are in the range of 15 and 270 g/denier (gpd), respectively, for 30 wt % (weight percent prior to sulfonation) SPAN composite fiber. Room-temperature dc conductivity σ_{RT} varies from 7.8×10^{-5} to 1.5×10^{-1} S/cm, increasing with increasing wt % polyaniline (PAn) and spin stretch factor (SSF). The temperature-dependent conductivity follows the quasi-one-dimensional variable range hopping (Q1D VRH) model: $\sigma_{dc}(T) = \sigma_0 \exp[-(T_0/T)^{\gamma}]$, where $\gamma \sim 0.5$ and σ_0 is a constant. T_0 is 4.3×10^4 to 2.9×10^4 K, respectively, for 10 and 30 wt % PAn. The σ_{mw} of the fiber with the same SSF 7.0 but a 30/70 PAn/PPD-T ratio shows a typical temperature dependence for materials for which the hopping conduction mechanism is dominant. There is a larger difference between the σ_{dc} and σ_{mw} following adjustment for the PAn/PPD-T ratio for 10/90 than for 30/70 as expected from lower conductivity. The similar T_0 with different σ_{RT} for samples having the same PAn/PPD-T ratio but different SSF suggests that spin stretching leads to the merging or alignment of the microfibers of SPAN followed by interconnection to each other without significant changes within the individual SPAN microfiber. The densities of Curie spins are ∼ 0.055 and 0.0074 spins/2-ring aniline repeat unit, respectively, for 30 and 10 wt %. The density of states at the Fermi level $N(E_F)$ is ∼ 0.64 and 0.57 states/eV·2-rings, ∼80% of what would be for PAn in which 50% of the rings are sulfonated, which is consistent with the sulfur analysis. Transport and magnetic data indicate an improved conduction in fiber samples compared with powder samples due to better alignment caused by spin stretching. These results suggest the formation of polarons and a conducting band based on the polaron energy level, consistent with earlier reported experimental results and models for 50% and 75% SPAN.

1. Introduction

Polyaniline consists of a large family of polymers which exist in three different discrete oxidation states at the molecular level: leucoemeraldine, emeraldine, and pernigraniline.[1] The emeraldine base form of polyaniline (PAn-EB) can be rendered electrically conductive through doping with a protonic acid. For practical applications, such as fibers, one would like to have their tensile properties as high as the polymer can provide. It is also desirable to have acid dopants permanently attached to the polyaniline for imparting electrical conductivity.

Fiber spinning coupled with heat drawing is a common processing technique for obtaining high tensile properties. PAn-EB fibers spun from organic solutions[2−4] followed by heat stretching at 215 °C and doping with HCl have a maximum conductivity of 160 S/cm.[2] However, the HCl doping has a profoundly negative impact on fiber tensile properties. It reduces the tensile strength of the PAn fibers from 3.9 gpd (1 denier is defined as 1 g in weight per 9000 m length of fiber) to 1.4 gpd,[2] which is not a useful fiber strength. 3.9 gpd is equivalent to 413 MPa assuming that the fiber has a density of 1.2 g/cm^3. To avoid the negative effect due to acid doping, a PAn-EB/camphorsulfonic acid/*m*-cresol conductive solution was used[5] for continuous dry-jet spinning (also called air-gap spinning). The as-spun fiber is electrically conductive, having a conductivity of 203 S/cm at ambient conditions without post-spinning acid doping. However, the tensile strength and modulus of the fiber are only 0.2 gpd and 7.3 gpd, respectively, which are not useful mechanical properties for any practical applications.

On the basis of the work reported thus far on fibers made with a typical molecular weight[2,3,5] of PAn, it is not likely that high strength (>5 gpd) and high modulus (>50 gpd) conductive PAn fibers can be achieved without a second polymer to provide tensile properties. Electrically conductive blend fibers have been produced from a dilute isotropic solution of PAn and PPD-T in 98 wt % sulfuric acid.[6] However, the fiber with 25 wt % PAn has 2.2 gpd tensile strength, which is still not useful for a wide range of applications. The fiber also requires hydrochloric acid, HCl, doping to achieve a conductivity of 0.01 S/cm. In 1998, Hsu et al.[7] reported PAn composite fibers, PAn/PPD-T H_2SO_4, made from air-gap spinning of lyotropic polyaniline/poly(*p*-phenylene terephthalamide) sulfuric acid solutions. The PAn is finely dispersed around PPD-T domains oriented parallel to the fiber axis. The PAn is sulfonated during the processing and does not require external doping to render the fiber conductive. In this paper we present EPR spin susceptibility χ(T) and microwave frequency dielectric constant ϵ_{mw} that demonstrate the formation

* Corresponding author. Telephone: (614) 292-1133, Fax: (614) 292-3706, Electronic mail: epstein@ mps.ohio-state.edu.
[†] Department of Physics, The Ohio State University.
[‡] Chemical Physics Program, The Ohio State University.
[§] Department of Chemistry, The Ohio State University.
[||] DuPont Co.

10.1021/ma001509h CCC: $20.00
Published on Web 03/10/2001

Table 1. Mechanical Properties of Fibers as a Function of Spin Stretch Factor (SSF) and EB/PPD-T Ratio

fiber	EB/PPD-T (w/w)[a]	SSF	denier (*d*)/*T* (gpd[b])/*E* (%)/*M* (gpd)
A	30/70	7	2.3/15.4/5.9/276
B	30/70	2.8	4.9/15.2/5.5/290
C	10/90	7	1.9/25.5/6.0/409
D	10/90	2.8	4.6/23.5/7.0/331

[a] Weight ratio prior to sulfonation. [b] Gram per denier.

of a disorder-induced localization of electronic states producing a distribution of energy levels resulting in an energy band with a finite $N(E_F)$ with charge hopping among these levels. Charge transport properties, including dc and microwave frequency conductivity, are analyzed in terms of a quasi-one-dimensional variable range hopping (Q1D VRH) model, appropriate for the disorder-localized system.

2. Experimental Details

2.1. Preparation of SPAN/PPD-T Fibers. 2.1.1. Synthesis of Polyaniline (Emeraldine Base)−PAn-EB. First, 134.3 g of aniline, 194.4 g of HCl solution (37 wt % concentration) and 1350 g of deionized water were placed in a jacketed, two-liter glass reaction vessel. The vessel was continuously swept with a nitrogen gas stream while the solution was stirred using a twin-bladed, 3-in. diameter impeller. A coolant fluid, supplied by a chilling unit, was circulated through the reactor jacket to cool the aniline/HCl solution down to −3 °C. To the solution was added an aqueous solution containing 155 g of ammonium persulfate and 270 g of water, at a rate of 1.95 cm^3/min using a syringe pump. Following addition of the oxidant solution, the reaction liquid was continuously stirred and chilled at about −3 °C for 3.5 days. The reactor contents were then filtered using a Buchner funnel. The collected mass was slurried in water and refiltered. The washing was repeated several times. The polymer was then vacuum-dried before being neutralized twice by reslurrying the polymer powder in 0.15 M NH_4OH solution for 24 h during each neutralization. The neutralized polymer was dried before being washed with 1.5 L of methanol twice, followed by a final wash with acetone. The polymer was then dried, has an inherent viscosity of 1.3 (30 °C, 0.5 wt % in H_2SO_4), and is not electrically conductive since the as-synthesized polyaniline was neutralized with ammonium hydroxide.

2.1.2. 18.6 wt % PAn-EB/PPD-T H_2SO_4 Solution. Two 18.6 wt % PAn-EB/PPD-T (30/70 for fibers of type A and B and 10/90 for fibers of type C and D) anisotropic solutions were prepared by mixing emeraldine base prepared above with PPD-T and H_2SO_4 (concentration > 100%) at temperatures between 60 and 80 °C. The anisotropic dopes then were transferred to a spin cell for extrusion into fibers. The fibers were extruded from a 10-hole spinneret having orifice diameter of 0.076 mm (3 mil), passed through an air-gap, and finally entered an aqueous coagulation bath. The 10-filament yarn was thoroughly washed with deionized water and dried. The fibers do not lose conductivity even with extensive washing with a dilute aqueous ammonium hydroxide or sodium hydroxide solution and drying afterward. Sulfur analysis shows that resulting PAn has ~10 wt % sulfur, confirming that PAn is sulfonated during the solutioning and spinning. The sulfur wt % represents 0.8 sulfur per every two aniline rings in the sulfonated polyaniline. The mechanical properties of tenacity/percent elongation at break/modulus (*T*/*E*/*M*), denier, and spin stretch factor (SSF) of fiber samples of the four types designated as A, B, C and D, respectively, are presented in Table 1. The repeat units for PPD-T, EB, and 50% sulfonated polyaniline (50% SPAN) are shown in Figure 1.

2.2. Experimental Techniques. Electron paramagnetic resonance (EPR) measurements (9.5 GHz) were carried out on ~13 cm lengths of sample fibers using a Bruker ESP300E

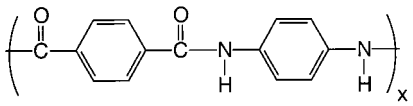

Poly(*p*-phenylene terephthalamide) (PPD-T)

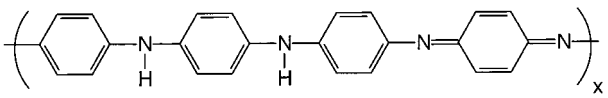

Polyaniline (PAn) - emeraldine base (EB) form

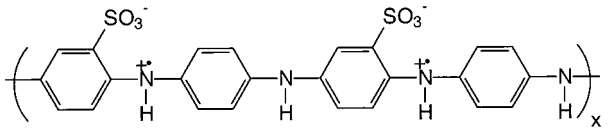

50% sulfonated polyaniline (50%SPAN)

Figure 1. Schematic repeat units for poly(*p*-phenylene terephthalamide (PPD-T), polyaniline (PAn)−emeraldine base (EB) form, and 50% sulfonated polyaniline (50% SPAN, self-doped state).

(Upgrade N) spectrometer and Oxford ESR900 cryostat under ITC503 temperature control. The resonance frequency of the incident radiation was verified with a Hewlett-Packard 5342A microwave frequency counter. The magnetic susceptibilities are calculated from the integrated intensity of EPR absorption and calibrated using a powdered crystalline $Cu^{II}SO_4 \cdot 5H_2O$ standard. The temperature-dependent dc conductivity and mw measurements at 6.5 GHz on fiber samples were performed utilizing the four-probe or two-probe and cavity perturbation[8−10] methods, respectively. Samples were contacted on the surface with gold wire using an Acheson 502 Electrodag in the four-probe method. For the cavity perturbation method, the sample was small enough to satisfy the depolarization condition.

3. Results and Discussion

3.1. Mechanical Properties. Table 1 shows tensile tenacity and modulus for 10 and 30 wt % PAn composite fibers. It is not surprising that both tenacity and modulus decrease substantially as the weight percentage of PAn increases since PAn is the non-stress-bearing component in the fiber. The tensile properties are from PPD-T, which is well-known for its ability in forming highly oriented fibers from lyotropic solutions. It is noted that the tenacity (15 gpd) and modulus (276 gpd) at 30 wt % PAn are much higher than the tenacity (2.2 gpd) and modulus (90 gpd) of PAn/PPD-T (25/75) fibers spun from an isotropic solution.[6]

3.2. Magnetic Properties. The magnetic susceptibilities of fibers of types A (○) and C (□) are plotted as $\chi(T) \times T$ vs T in Figure 2. The Curie constant ($\chi_C = C/T$, where C is the Curie constant and χ_C is the Curie susceptibility attributed to isolated spins) and Pauli susceptibility (χ_P is attributed to the formation of a partially filled energy band with a finite density of states at the Fermi level ($N(E_F)$) were determined by fitting the data to

$$\chi(T) \times T = \chi_P T + C$$

Using a regression analysis to fit a line to the data, the Curie constant is 5.85×10^{-4} and 2.12×10^{-4} emu·K/mol, respectively, for fiber types A and C. The density of Curie spins calculated from the Curie constant is ~

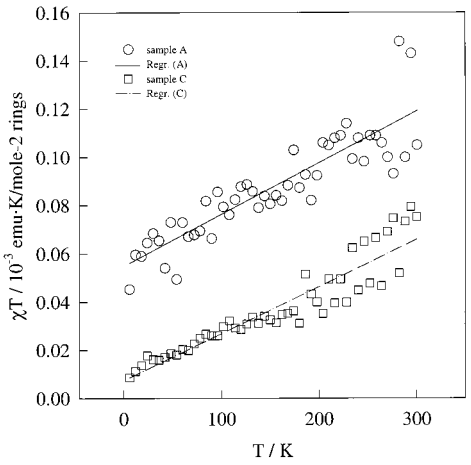

Figure 2. χT vs T as a function of temperature for fibers A (○) and C (□).

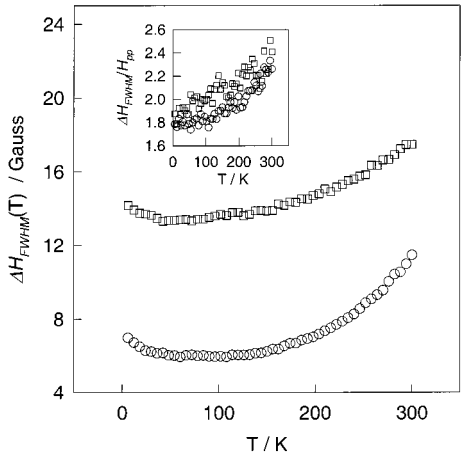

Figure 3. ΔH_{fwhm} vs T, for fibers A (○) and C (□). Left top inset shows temperature dependence of $\Delta H_{fwhm}/H_{pp}$.

0.055 and 0.0074 spins/2-ring aniline repeat unit (corresponding to the stoichiometry for fully doped emeraldine salt), on the order of the 0.02 spin/2-rings aniline repeat unit of 50% SPAN.[11] The Pauli susceptibility for the fiber, also determined by regression analysis, is $\sim 2.21 \times 10^{-5}$ and 1.95×10^{-5} emu/mol 2-rings, respectively. Using the equation $\chi_P = 2N_A\mu_B^2N(E_F)$, $N(E_F) \sim$ 0.64 and 0.57 states/eV·2-rings aniline for fibers of type A and C, respectively. These values are about 80% of that for 50% SPAN, ~0.8 states/eV·2-rings.[11] This is consistent with the sulfur analysis, which indicates that only ~40% of the PAn-EB rings are sulfonated. As developing a finite $N(E_F)$ requires an array of regions of ~50% sulfonated portions of PAn, this average sulfonation level suggests that there is some segregation of nonsulfonated PAn segments from 50% sulfonated regions within the PAn chains and/or fibrils.

For 50%,[11] 75%,[12] and 100%[13] SPANs, the temperature-dependent full-width at half-maximum line widths ΔH_{fwhm} are 0.3 (50% SPAN) to 1 G (75% and 100% SPAN). These ΔH_{fwhm} increase monotonically as the temperature is lowered, reaching ~5 G at ~5 K. In contrast, the magnitudes of ΔH_{fwhm} for SPAN/PPD-T fibers are much larger and the temperature dependence has a minimum as the temperature is lowered, Figure 3. The inset shows $\Delta H_{fwhm}/H_{pp}$ where H_{pp} is the peak-to-peak value of the EPR absorption spectra. This indicates that spins in the fiber samples are in relatively delocalized states at low temperature with $\Delta H_{fwhm}/H_{pp}$-

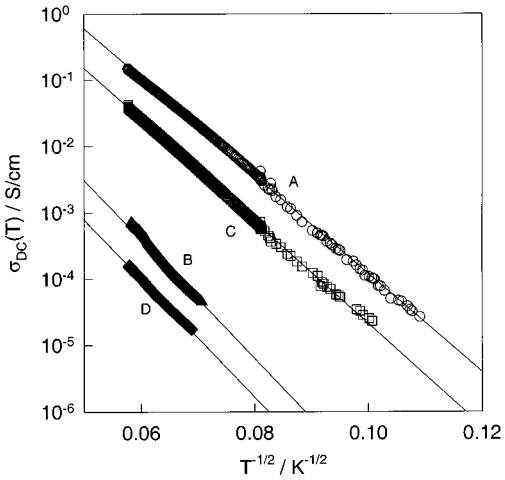

Figure 4. σ_{dc} of fibers: A (○), B (△), C (□), and D (◇).

($T \rightarrow 0$ K) ~ 1.8, close to the value for Lorentzian shape, 1.73. With increasing temperature $\Delta H_{fwhm}/H_{pp}$ increases toward unusual larger values. While $N(E_F)$ is consistent with earlier works[11−13] on partially sulfonated polyaniline and the density of Curie spins suggests relatively few localized electrons that are not well-coupled to the weakly localized electrons that form $N(E_F)$ (vide supra), the EPR line width is anomalous in its magnitude, shape and temperature dependence. Given that the line width is even larger for the 10/90 fibers as compared with the 30/70 fibers and that the 10/90 fibers appear to have the sulfonated polyaniline separated into thinner striations (<~20 nm) embedded in PPD-T as compared to the 30/70 fibers (<~40 nm),[7] we propose that the relatively large EPR line widths of these fiber types are due to interaction between the spins in the SPAN with PPD-T at the surface of the striations. The thinner striations of the 10/90 fibers would have a larger fraction of the polyaniline layers "in contact" with the PPD-T. It is suggested that increased diffusion of the spins to the surface of the polyaniline layers is the origin of the increasing line width with increasing temperature for $T > 100$ K. The increase in line width with decreasing T for $T < 100$ K likely originates from increasing spin localization.

The EPR line shapes are Lorentzian-like near the center, becoming distorted into the wings beyond the expected value of $\sqrt{3}$ for $\Delta H_{fwhm}/H_{pp}$. The degree of deviation from Lorentzian behavior increases with increasing temperature for both fiber types. The deviation is more pronounced in the 10/90 fibers again suggesting the role of interaction with the PPD-T in establishing the line shapes.

3.3. Charge Transport: Dc Conductivity and Microwave Properties. As shown in Figure 4, the σ_{dc} is well fit by

$$\sigma_{dc}(T) = \sigma_0 \exp[-(T_0/T)^{\gamma}]$$

Assuming Q1D VRH,[10,14] $T_0 = 8\alpha/(zN(E_F)k_B)$, where α^{-1} is the localization length, k_B is the Boltzmann constant, and z is the number of the nearest neighbor chains. σ_{dc} is dominated by charge conduction through the least conducting (most disordered) regions, especially in the case of the insulating side of the metal−insulator transition.[15]

σ_{RT}, T_0 from the Q1D VRH model, the fiber diameter, and SSF of fiber samples are summarized in Table 2.

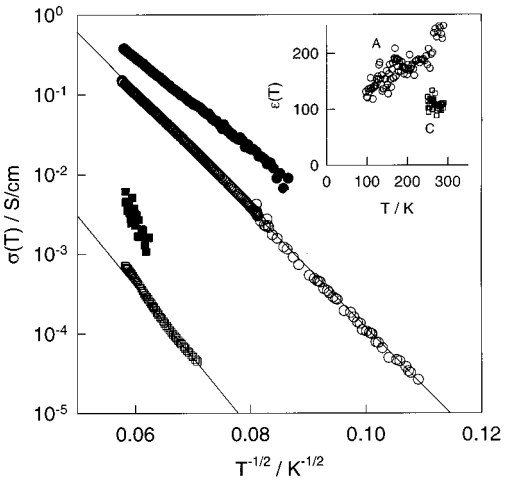

Figure 5. σ_{dc} vs $T^{-1/2}$ of fibers A(○) and B(△), and the σ_{mw} of sample A (●) and sample C (■). Right above inset shows the ϵ_{mw} for fibers A (○) and C (□).

Table 2. Summary of σ_{RT}, T_0, Diameter, and SSF of Fiber Samples

fiber	σ_{RT} (S/cm)	T_0 (K)	diameter (μm)	SSF
A	1.5×10^{-1}	2.9×10^4	14.2	7
B	4.0×10^{-2}	3.2×10^4	23.9	2.8
C	7.8×10^{-4}	4.3×10^4	13.5	7
D	7.8×10^{-5}	4.2×10^4	22.4	2.8

Fiber type A has the highest room-temperature conductivity ~0.15 S/cm (~0.5 S/cm^2 if the conductivity is normalized for the fraction of the cross-sectional area comprised of PAn) with $T_0 \sim 2.9 \times 10^4$ K, which is consistent with its largest SSF 7.0 and highest PAn/PPD-T ratio, 30/70, as shown in Table 1. Although fiber types A and B only have 30 wt % EB prior to sulfonation, their T_0 values are smaller than that (3.9×10^4 K) of compressed powder pellets of 50% SPAN.[11] Their conductivity is also higher than that ($\sigma_{RT} \sim 0.1$ S/cm)[11] of compressed powder pellets, which demonstrates that PAn chain alignment facilitates electrical conduction in the fiber. The T_0 values are somewhat larger than that (2.5×10^4 K) of a compressed powder pellet of 75% SPAN which has $\sigma_{RT} \sim 1$ S/cm.[12] For fiber types C and D, both of which have 10 wt % PAn prior to sulfonation, $\sigma_{RT} \approx 7.4 \times 10^{-4}$ and 7.4×10^{-5} S/cm (normalizing to $\sim 8 \times 10^{-3}$ and 8×10^{-4} S/cm, respectively, when the presence of only 10 wt % PAn is taken into account) are lower than σ_{RT} (0.02 S/cm) of a compressed powder pellet of 100% SPAN powder[13] or poly(*o*-toluidine)−HCl (POT-HCl) fiber.[16] The T_0 values are close to the 3.9×10^4 K of the 50% SPAN or POT-HCl fiber. Comparing fiber types A and B with the same PAn/PPD-T ratio (30/70) but different SSF, T_0 of the two fiber types are close to each other. However, σ_{RT} of fiber type A with larger SSF is larger by a factor of 4. This is also the case with fiber types C and D with the same PAn/PPD-T ratio 10/90 but different SSF. This suggests that spin stretching leads to the merging or alignment of the SPAN microfibers followed by interconnection to each other without any substantial change within the SPAN microfibers of a single filament.

As shown in Figure 5, the σ_{mw} of fiber type A is 3.7×10^{-1} S/cm, about two times larger than its dc value. σ_{mw} is weaker than σ_{dc} as is expected for pairwise hopping.[10,14] The ϵ_{mw} of fibers of type A shows a weak temperature dependence, decreasing from ~200 ± 20 at room temperature to ~120 ± 10 at 100 K with decreasing temperature. The room-temperature dielectric constant of ~200 ± 20 is much larger than that of 100% SPAN.[13] A larger dielectric constant and smaller T_0 than for 50% SPAN can be understood in terms of formation of larger delocalization regions in fibers than in compressed powders due to the alignment of microfibers. The smaller T_0 but still smaller σ_{RT} in the SPAN/PPD-T fiber compared with those in the 50% SPAN compressed powder sample are likely due to PPD-T reducing charge transport between many other SPAN regions. The σ_{mw} of fiber type C with the same SSF 7.0 and smaller EB loading is $\sim 5 \times 10^{-3}$ S/cm, almost 1 order of magnitude larger than the dc value. This is also due to the sum of a dc term and an additional contribution from pairwise hopping as in fibers of type A. The stronger temperature dependence of the σ_{mw} than σ_{dc} is unusual and may reflect discontinuities within the doped regions, leading to lower conductivity or errors in the cavity perturbation technique analysis. The dielectric constant of fibers of type C at room temperature is ~100 ± 10 and is nearly temperature-independent in the region shown.

The relatively small T_0 and large dielectric constant with rather small σ_{RT} compared with pressed pellets of 100% SPAN powders[17] suggests that fiber samples are better aligned compared with powder samples due to spin stretching with still incomplete alignment overall. The effective localization length can also be calculated from the temperature dependence of the σ_{dc} using the relation $T_0 = 8\alpha/(zN(E_F)k_B)$. Using $N(E_F) \sim 0.64$ and 0.57 states/eV-2 rings from the EPR measurements, $z \sim 4$, and $T_0 = 2.9 \times 10^4$ and 4.3×10^4 K from σ_{dc} measurements, the localization lengths α^{-1} are determined to be ~10 and 8 Å for fiber types A and C, respectively, which is larger than those for 50%[11] or 75%[12] SPAN powders, ~6 Å. The relatively small T_0, large dielectric constant, and $\Delta H_{fwhm}/H_{pp}$ at low temperature indicate a weakly localized state in SPAN/PPD-T fibers, suggesting the formation of a partially filled energy band (based on the polaron energy levels[18]) with disorder. The insulating PPD-T causes the separation of conducting PAn regions. This results in lower room temperature and anomalous EPR line width and temperature dependence.

4. Conclusion

Tensile tenacity and modulus of SPAN/PPD-T fibers are very high due to the presence of PPD-T which results in highly oriented polymer chains from air-gap spinning of lyotropic solutions. Temperature-dependent transport and magnetic properties suggest a Q1D VRH conduction mechanism, indicating formation of a weakly localized conduction band in the fibers. The similar T_0 with different σ_{RT} for the fiber types having the same SPAN/PPD-T ratio but different SSF supports the point that spin stretching leads to the merging or alignment of the microfibers of SPAN followed by interconnection to each other without any change of order within the microfibers of a single filament. Smaller T_0, larger ϵ_{mw}, and Lorentzian-like $\Delta H_{fwhm}/H_{pp}$ at low temperature compared with those for compressed powders of SPAN reveal a less localized state in the fibers, demonstrating an improved conduction in the fiber samples compared with the compressed powder sample because of better alignment resulting from spin stretching.

Acknowledgment. This research was supported in part by ONR.

References and Notes

(1) MacDiarmid, A. G.; Epstein, A. J. *Faraday Discuss. Chem. Soc.* **1989**, *88*, 317−332.
(2) Hsu, C.-H.; Cohen, J. D.; Tietz, R. F. *Synth. Met.* **1993**, *59*, 37−41.
(3) Wang, Y. Z.; Joo, J.; Hsu, C.-H.; Pouget, J. P.; Epstein, A. J. *Macromolecules* **1994**, *27*, 5871−5876.
(4) Tzou, K. T.; Gregory, R. V. *Polym. Prepr.* **1994**, *35* (1), 245−246.
(5) Hsu, C.-H.; Epstein, A. J. *Annu. Technol. Conf.—Soc. Plast. Eng.* **1996**, *54*, 1353−1357.
(6) Andreatta, A.; Heeger, A. J.; Smith, P. *Polym. Commun.* **1990**, *31*, 275−278.
(7) Hsu, C.-H.; Shih, H.; Subramoney, S.; Epstein, A. J. *Synth. Met.* **1999**, *101*, 677−680.
(8) Javadi, H. H.; Cromack, K. R.; MacDiarmid, A. G.; Epstein, A. J. *Phys. Rev. B* **1989**, *39*, 3579−3584.
(9) Buranov, L. I.; Shchegolev, I. F. *Prib. Tekh. Eksp.* **1971**, *2*, 171−173 [*Instrum. Exp. Tech.* **1971**, *14*, 528−530].
(10) Wang, Z. H.; Scherr, E. M.; MacDiarmid, A. G.; Epstein, A. J. *Phys. Rev. B* **1992**, *45*, 4190−4202.
(11) Yue, J.; Wang, Z. H.; Cromack, K. R.; Epstein, A. J.; MacDiarmid, A. G. *J. Am. Chem. Soc.* **1991**, *113*, 2665−2671.
(12) Wei, X.-L.; Wang, Y. Z.; Long, S. M.; Bobeczko, C.; Epstein, A. J. *J. Am. Chem. Soc.* **1996**, *118*, 2545−2555.
(13) Lee, W.; Du, G.; Long, S. M.; Epstein, A. J.; Shimizu, S.; Saitoh, T.; Uzawa, M. *Synth. Met.* **1997**, *84*, 807−808.
(14) Mott, N. F.; Davis, E. A. *Electronic Processes in Non-Crystalline Materials*, 2nd ed.; Clarendon Press: Oxford, England, 1979.
(15) Kohlman, R. S.; Epstein, A. J. In *Handbook of Conducting Polymers*, 2nd ed.; Skotheim, T. A., Elsenbaumer, R. L., Reynolds, J. R., Eds.; Marcel Dekker: New York, 1998; Chapter 3, pp 85−121.
(16) Wang, Y. Z.; Joo, J.; Hsu, C.-H.; Epstein, A. J. *Synth. Met.* **1995**, *68*, 207−211.
(17) Lee, W.-P.; Brenneman, K. R.; Long, S. M.; Saprigin, A.; Epstein, A. J.; Shimizu, S.; Saitoh, T.; Uzawa, M. Submitted for publication.
(18) Ginder, J. M.; Richter, A. F.; MacDiarmid, A. G.; Epstein, A. J. *Solid State Commun.* **1987**, *63*, 97−101.

MA001509H